AD-A046 237 R AND D ASSOCIATES MARINA DEL REY CALIF F/G 17/2.1
EFFECT OF A CYLINDRICALLY-SYMMETRIC IONOSPHERIC DISTURBANCE ON --ETC(U)
JUN 77 C GREIFINGER, P GREIFINGER DNA001-76-C-0001
UNCLASSIFIED RDA-TR-2005-002 DNA-4339T NL

1 OF 1
ADA
046237

END
DATE
FILMED
12-77
DDC

DNA 4339T

EFFECT OF A CYLINDRICALLY-SYMMETRIC IONOSPHERIC DISTURBANCE ON ELF PROPAGATION IN THE EARTH-IONOSPHERE WAVEGUIDE.

R&D Associates
P.O. Box 9695
Marina del Rey, California 90291

10 June 1977

Topical Report

CONTRACT No. DNA 001-76-C-0001

39 p.

Carl Greifinger
Phyliss Greifinger

THIS WORK SPONSORED BY THE DEFENSE NUCLEAR AGENCY
UNDER RDT&E RMSS CODE B310076464 P99QAXDB00117 H2590D.

Prepared for
Director
DEFENSE NUCLEAR AGENCY
Washington, D. C. 20305

Destroy this report when it is no longer needed. Do not return to sender.

The views and conclusions contained in this document are those of the authors and should not be interpreted as necessarily representing the official policies, either expressed or implied, of the Defense Nuclear Agency or the United States Government.

UNCLASSIFIED

SECURITY CLASSIFICATION OF THIS PAGE *(When Data Entered)*

REPORT DOCUMENTATION PAGE		READ INSTRUCTIONS BEFORE COMPLETING FORM
1. REPORT NUMBER DNA 4339T	2. GOVT ACCESSION NO.	3. RECIPIENT'S CATALOG NUMBER
4. TITLE *(and Subtitle)* EFFECT OF A CYLINDRICALLY-SYMMETRIC IONOSPHERIC DISTURBANCE ON ELF PROPAGATION IN THE EARTH-IONOSPHERE WAVEGUIDE		5. TYPE OF REPORT & PERIOD COVERED Topical Report 6. PERFORMING ORG. REPORT NUMBER RDA-TR-2005-002
7. AUTHOR(s) Carl Greifinger Phyliss Greifinger		8. CONTRACT OR GRANT NUMBER(s) DNA 001-76-C-0001
9. PERFORMING ORGANIZATION NAME AND ADDRESS R & D Associates P.O. Box 9695 Marina del Rey, California 90291		10. PROGRAM ELEMENT, PROJECT, TASK AREA & WORK UNIT NUMBERS NWED Subtask P99QAXDB001-17
11. CONTROLLING OFFICE NAME AND ADDRESS Director Defense Nuclear Agency Washington, D.C. 20305		12. REPORT DATE 10 June 1977 13. NUMBER OF PAGES 42
14. MONITORING AGENCY NAME & ADDRESS *(if different from Controlling Office)*		15. SECURITY CLASS *(of this report)* UNCLASSIFIED 15a. DECLASSIFICATION DOWNGRADING SCHEDULE

16. DISTRIBUTION STATEMENT *(of this Report)*

Approved for public release; distribution unlimited.

17. DISTRIBUTION STATEMENT *(of the abstract entered in Block 20, if different from Report)*

18. SUPPLEMENTARY NOTES

This work sponsored by the Defense Nuclear Agency under RDT&E RMSS Code B310076464 P99QAXDB00117 H2590D.

19. KEY WORDS *(Continue on reverse side if necessary and identify by block number)*

20. ABSTRACT *(Continue on reverse side if necessary and identify by block number)*

A nuclear explosion in the earth's inonosphere produces a depression in the ionosphere that is approximately cylindrically symmetric. In this paper, a method is developed for calculating the change in amplitude and phase at a receiver of an ELF (extremely low frequency) radio wave in the presence of such a localized, cylindrically-symmetric disturbance. Numerical results are obtained for the particular configuration where the center of the disturbance is directly above the transmitter-receiver path.

DD FORM 1 JAN 73 1473 EDITION OF 1 NOV 65 IS OBSOLETE

(cont on p 1473B)

UNCLASSIFIED

SECURITY CLASSIFICATION OF THIS PAGE *(When Data Entered)*

20. ABSTRACT (Continued)

The attenuation from one edge of the disturbance to the opposite edge is found to be only about half of that calculated by the two-dimensional WKB approximation usually employed in such problems.

SUMMARY AND CONCLUSIONS

An accurate full-wave method for determining the effect on ELF radio propagation of a localized, cylindrically-symmetric disturbance has been developed. Application of this method to the disturbance produced by a high-altitude nuclear explosion gives, when the transmitter is outside of the disturbed region, greater attenuation in most of this region than does the two-dimensional WKB approximation used by previous workers, but less attenuation at the far edge of the region. For example, 10 min after a typical megaton-range, high-altitude nuclear explosion, the signal level at the far edge is calculated to be 3 dB below that before the burst, while the two-dimensional approximation gives a 7-dB decrease. Such differences are very important for ELF systems whose enormous power requirements may necessitate operation at minimal signal-to-noise ratios.

The analysis in this report also shows that ELF fields at the ground are sensitive to the details of ionospheric conductivity profiles only in two rather limited altitude ranges. The lower of these is the altitude range where the conduction and displacement currents are comparable. The upper region is where the conductivity scale height is comparable with the skin depth. Future effort in obtaining improved conductivity profiles for ELF propagation calculations should therefore focus on these two altitude ranges.

TABLE OF CONTENTS

SECTION I

INTRODUCTION

The purpose of this report is to present a method for determining the effect on ELF (extremely low frequency) radio communication of a localized, cylindrically-symmetric ionospheric disturbance, such as would be produced by a solar proton event or a high-altitude nuclear burst. At ELF, wavelengths are frequently comparable with the dimensions of ionospheric disturbances, either natural or artificial. Consequently, approximate methods for handling such problems at VLF, such as the WKB approximation or the Fresnel diffraction model of Crombie [1], are not applicable at ELF. At these lower frequencies, it becomes necessary to work with full-wave solutions of Maxwell's equations in the earth-ionosphere waveguide.

There are well-known techniques for obtaining full-wave solutions for an earth-ionosphere waveguide in which there is inhomogeneity in only the vertical direction [2-4]. For certain idealized conductivity profiles, analytic solutions are possible. However, for more realistic profiles, solutions can be obtained only by numerical methods. Either procedure involves the solution of an eigenvalue equation, each eigenvalue and corresponding eigenfunction corresponding to a particular waveguide mode. The electromagnetic field radiated by any source in the waveguide can be expressed as a superposition of waveguide modes, with relative amplitudes depending on the nature of the source. At ELF, this representation of the electromagnetic field is especially convenient because only the lowest, or TEM, mode is nonevanescent in the earth-ionosphere waveguide. At distances from a source exceeding 2 or 3 times the height of the waveguide, only its TEM component remains.

The source of particular interest here is a horizontal electric dipole antenna located at or near the ground. For a

horizontal dipole with current moment $Id\ell$, oriented along the direction $\alpha = 0$, and varying with time as $e^{-i\omega t}$, the vector potential for the TEM mode is

$$A_z = \frac{\mu_o Id\ell}{2n_g} \Lambda_o \cos\alpha \; f_o(z) H_1^{(1)}(kS_o r) \qquad (1\text{-}1)$$

where $k = \omega/c$ is the wave number, n_g is the index of refraction of the ground, z is the height above the ground, and r is the horizontal distance from the source. The quantity S_o is an eigenvalue characterizing the TEM mode and $f_o(z)$ is the corresponding eigenfunction normalized to $f_o = 1$ at the ground ("height-gain function"). The quantity Λ_o, which has the dimensions of a reciprocal length, is known as the "excitation factor."

Sufficiently far from the source, the Hankel function in Equation (1-1) may be approximated by its large argument expansion, which has the form

$$H_1^{(1)}(kS_o r) \rightarrow \frac{1}{r^{1/2}} e^{ikS_o r} \qquad (1\text{-}2)$$

From this it can be seen that the real part of the (complex) eigenvalue S_o is the reciprocal of the horizontal phase velocity in units of c. The imaginary part of S_o is related to the horizontal attenuation rate by

$$\alpha = 8.7 \times 10^3 \; k\,\mathrm{Im}(S_o) \quad \mathrm{dB/(1000\ km)} \qquad (1\text{-}3)$$

where k is the wave number in km^{-1}.

When the properties of the waveguide are laterally, as well as vertically, inhomogeneous, such as in the presence of a localized disturbance, the vector potential no longer has the simple form of Equation (1-1). However, if the scale

lengths for the lateral gradients are much larger than those for the vertical gradients, which is almost always the case, it can be expected that the vertical variation of the vector potential will be determined primarily by the local ionosphere. The lateral variation of the vector potential at the ground is then governed by a two-dimensional Schroedinger wave equation in which the effects of the localized disturbance appear in the form of a complex localized potential. The problem then reduces to the determination of the scattering from such a potential. These concepts form the basis of the theory which will be developed in the following sections.

A related approach to the problem has been developed by ilcox [5]. He presents a descriptive semiquantitative method or partial wave scattering from a cylindrically-symmetric potential from which upper bounds are obtainable on the absolute magnitude of scattering and absorption of ELF waves in a horizontally perturbed earth-ionosphere waveguide. The method presented here allows a calculation of the electromagnetic field everywhere in such a waveguide.

SECTION II

EFFECT OF LATERAL GRADIENTS ON TEM MODE

The equations which govern electromagnetic propagation in the earth-ionosphere waveguide are Maxwell's equations for a conducting medium together with a generalized Ohm's law

$$\vec{j} = \sigma\vec{E} + \vec{j}_s \qquad (2\text{-}1)$$

where $\vec{j}_s$ is the source current density. Due to the presence of the earth's magnetic field, the medium is anisotropic and the conductivity σ is in general a tensor. However, below about 70 km magnetic effects become unimportant and the medium is essentially isotropic. The conductivity below this altitude can therefore be considered a scalar. It will be shown later that the TEM field radiated by a source in the waveguide falls off very rapidly above the altitude at which the skin depth becomes comparable with the local conductivity scale height. In a nuclear environment, this altitude is generally below 70 km. For ambient ionospheric conditions, this altitude is near 70 km in the daytime but above 70 km at night. In the following, it will be assumed that the ambient ionosphere is a daytime one, so that magnetic effects may be neglected in the undisturbed as well as the disturbed region of the ionosphere.

The case to be considered is that of a localized cylindrically symmetric disturbance of an otherwise laterally homogeneous daytime ionosphere. It is convenient to use a cylindrical coordinate system (ρ,ϕ,z) about the axis of the disturbance, with the origin at the ground. With the above assumptions, and an assumed time dependence $e^{-i\omega t}$, Maxwell's equations become

$$\vec{\nabla} \times \vec{E} = i\omega\vec{B} \tag{2-2}$$

$$\vec{\nabla} \times \vec{B} = \mu_o[\sigma(\rho,z) - i\varepsilon_o\omega]\vec{E} + \mu_o\vec{j}_s \tag{2-3}$$

The second of these may be written

$$\vec{\nabla} \times \vec{B} = -\frac{in^2(\rho,z)k^2}{\omega}\vec{E} + \mu_o\vec{j}_s \tag{2-4}$$

where $k = \omega/c$ is the free-space wave number and

$$n^2(\rho,z) = \left[1 + \frac{i\sigma(\rho,z)}{\varepsilon_o\omega}\right] \tag{2-5}$$

is the square of the local index of refraction.

It is convenient to express the fields in terms of a vector potential $\vec{A}$ and a scalar potential ψ. Thus one writes, in the usual manner,

$$\vec{B} = \vec{\nabla} \times \vec{A} \tag{2-6}$$

$$\vec{E} = \vec{\nabla}\psi + i\omega\vec{A} \tag{2-7}$$

Substitution of Equation (2-6) and (2-7) into Equation (2-4) leads to

$$\vec{\nabla} \times \vec{\nabla} \times \vec{A} = [\vec{\nabla}(\vec{\nabla}\cdot\vec{A}) - \nabla^2\vec{A}] = \frac{n^2}{i\omega}k^2(\vec{\nabla}\psi + i\omega\vec{A}) + \mu_o\vec{j}_s \tag{2-8}$$

If the gauge of $\vec{A}$ is chosen to satisfy the condition

$$\frac{i\omega}{n^2}\vec{\nabla}\cdot\vec{A} = k^2\psi \tag{2-9}$$

the preceding equation becomes

$$\nabla^2\vec{A} + n^2(\vec{\nabla}\cdot\vec{A})\vec{\nabla}\,\frac{1}{n^2} + n^2k^2\vec{A} = -\mu_o\vec{j}_s \qquad (2\text{-}10)$$

For a horizontal dipole source, $\vec{A}$ has components in the direction of $\vec{j}_s$ and in the z-direction. However, if lateral gradients of n^2 are neglected compared with vertical gradients, only the z-component of $\vec{A}$ remains finite at distances from the source exceeding the thickness of the waveguide. Thus, for such distances, Equation (2-10) with appropriate boundary conditions can be satisfied by a vector potential of the form

$$\vec{A} = (0,0,A_z) \qquad (2\text{-}11)$$

The wave equation then reduces to

$$\frac{\partial}{\partial z}\left(\frac{1}{n^2}\,\frac{\partial A_z}{\partial z}\right) + \frac{1}{n^2}\,\nabla_\perp^2 A_z + k^2A_z = 0 \qquad (2\text{-}12)$$

where

$$\nabla_\perp^2 = \frac{1}{\rho}\,\frac{\partial}{\partial\rho}\left(\rho\frac{\partial}{\partial\rho}\right) + \frac{1}{\rho^2}\,\frac{\partial^2}{\partial\phi^2} \qquad (2\text{-}13)$$

is the transverse Laplacian.

In the case of a laterally homogeneous medium, where n^2 is a function only of z, the vertical and transverse parts of Equation (2-12) can be separated. Thus, one writes

$$A_z(\rho,\phi,z) = g(\rho,\phi)f(z) \qquad (2\text{-}14)$$

which leads to the two eigenvalue equations

$$\nabla_t^2 g + k^2 S^2 g = 0 \qquad \text{(Bessel's equation)} \qquad (2\text{-}15)$$

$$\frac{d}{dz}\left(\frac{1}{n^2}\frac{df}{dz}\right) + k^2\left(1 - \frac{S^2}{n^2}\right) f = 0 \qquad (2\text{-}16)$$

where S is a constant. The various TM modes, of which the TEM is the lowest, are solutions of this form satisfying appropriate boundary conditions. The only constraint on the solutions of Equation (2-15) is the radiation condition, which requires outgoing waves at large lateral distances. Such solutions exist for any value of the parameter S. However, the function f(z) must satisfy two boundary conditions, one at the ground and the other at large altitude. These can be satisfied simultaneously only for certain, in general complex, values of S. The eigenfunctions corresponding to these eigenvalues are the TM modes of the waveguide.

In the presence of lateral gradients, a separation of Equation (2-12) in the form of Equation (2-14) is not possible. However, since the scale lengths for the horizontal variations of the ionospheric index of refraction are a few orders of magnitude larger than those for vertical variations, it seems reasonable to assume that the vertical dependence of the vector potential is determined primarily by the local ionosphere. Thus, it is assumed by analogy with Equation (2-16) that the vertical variation of A_z is governed by the equation

$$\frac{\partial}{\partial z}\left(\frac{1}{n^2(\rho,z)}\frac{\partial A_z}{\partial z}\right) + k^2\left(1 - \frac{S^2(\rho)}{n^2(\rho,z)}\right) A_z = 0 \qquad (2\text{-}17)$$

where $S^2(\rho)$ is the eigenvalue corresponding to a laterally homogeneous waveguide with the vertical conductivity profile that exists at ρ.

Near the perfectly conducting ground, A_z has the form

$$A_z = g(\rho,\phi) + G(\rho,\phi)\ \frac{z^2}{2} + \ldots \qquad (2\text{-}18)$$

Since $n^2 = 1$ near the ground, Eqs. (2-12), (2-17) and (2-18) give

$$G(\rho,\phi) = -\ k^2\left(1-S^2(\rho)\right) g(\rho,\phi) \qquad (2\text{-}19)$$

$$\nabla_\perp^2\ g(\rho,\phi) + k^2 S^2(\rho)\ g(\rho,\phi) = 0 \qquad (2\text{-}20)$$

The solution of the problem requires first a determination of $S^2(\rho)$, by a solution of Equation (2-17) at as many lateral distances as necessary, followed by an integration of Equation (2-20). The first step can of course by carried out by one of the techniques mentioned in the introduction for the numerical solution of an eigenvalue equation. However, this could involve a large amount of computation, which is probably unwarranted in view of the considerable uncertainties in ionospheric conductivity profiles. As an alternative, an approximate method for determining $S^2(\rho)$, involving very little calculation, will be presented in the next section. It will be shown that approximate eigenvalues obtained in this manner agree very well with those calculated by full wave solutions, and are therefore quite adequate for the present purposes.

SECTION III

APPROXIMATE METHOD FOR EIGENVALUE DETERMINATION

The method for determining approximate eigenvalues depends on the fact, to be demonstrated presently, that the eigenvalue depends on the details of the conductivity profile only in two limited altitude ranges. The lower of these is the neighborhood of the altitude h_o at which $\sigma = \varepsilon_o\omega$. The upper region is the neighborhood of the altitude h_1 at which $\sigma = (4\mu_o\omega\zeta_1^2)^{-1}$, where ζ_1 is the conductivity scale height at the altitude h_1. The method consists first of approximating the conductivity in each region by an exponential with the local conductivity scale height. Two analytic solutions of Maxwell's equations are then obtained. One obeys the proper boundary condition as $z \to \infty$ and is valid in the altitude range $h_o << z < \infty$. The other obeys the appropriate boundary condition at the ground and is valid in the altitude range $0 < z << h_1$. There is a region $h_o << z << h_1$ where both solutions are valid. The eigenvalue $S(\rho)$, which appears as a parameter in these solutions, is determined by requiring that the solutions agree in the overlap region.

The basic equations are Equation (2-9), which becomes

$$\frac{i\omega}{n^2}\frac{\partial A_z}{\partial z} = k^2\psi \qquad (3\text{-}1)$$

and Equation (2-17). These equations must be solved subject to appropriate boundary conditions at the ground and at large altitude. At ELF, the ground can be considered perfectly conducting, and the horizontal electric field at the ground must therefore vanish. At very large altitudes, the solution is required by the radiation condition to contain only upgoing waves.

The conductivity σ is an increasing function of altitude. The altitude h_o at which the conduction current becomes equal to the displacement current, i.e., at which $\sigma(h_o) = \varepsilon_o\omega$, roughly marks the lower boundary of the ionosphere. For altitudes $z >> h_o$,

$$n^2 \approx \frac{i\sigma}{\varepsilon_o\omega} >> 1 \tag{3-2}$$

and Equation (2-17) becomes approximately

$$\frac{\partial}{\partial z}\left(\frac{\varepsilon_o\omega}{i\sigma}\frac{\partial A_z}{\partial z}\right) + k^2 A_z = 0 \tag{3-3}$$

Combined with Equation (3-1), this leads to the wave equation

$$\frac{\partial^2\psi}{\partial z^2} + i\mu_o\sigma\omega\psi = 0 \tag{3-4}$$

In any limited altitude range, the conductivity may be approximated by an exponential, with a scale height appropriate to that altitude. Near a height h_1 to be determined shortly, the conductivity may therefore be written

$$\sigma(z,\rho) = \sigma_1(h_1,\rho)e^{(z-h_1)/\zeta_1} \tag{3-5}$$

where both h_1 and ζ_1 are functions of ρ.

In the vicinity of h_1, a change of variable to

$$y = e^{i\pi/4}\, e^{(z-h_1)/2\zeta_1} \tag{3-6}$$

allows Equation (3-4) to be transformed to

$$y^2 \frac{\partial^2 \psi}{\partial y^2} + y \frac{\partial \psi}{\partial y} + 4\mu_o \sigma_1 \omega \zeta_1^2 y^2 \psi = 0 \qquad (3\text{-}7)$$

If one chooses h_1 to be that altitude at which

$$2\zeta_1 (\mu_o \sigma_1 \omega)^{1/2} = 1, \qquad (3\text{-}8)$$

Equation (3-7) takes the canonical form of Bessel's equation. The solution corresponding to outgoing waves at large altitude is

$$\psi = f(\rho)\ H_o^{(1)} \left[e^{i\pi/4}\ e^{(z-h_1)/2\zeta_1} \right] \qquad (3\text{-}9)$$

Above h_1, which is the altitude at which the skin depth equals twice the conductivity scale height, the potentials fall to zero extremely rapidly. Thus, h_1 represents the upper boundary of the waveguide, where ultimate reflection takes place. It will be seen later that significant reflection also takes place at the altitude h_o.

For altitudes $z << h_1$, the Hankel function in Equation (3-9) may be approximated by its small argument expansion. The scalar potential in the altitude range $h_o << z << h_1$ thus takes the form

$$\psi \longrightarrow F(\rho) \left[z - h_1 - \frac{i\pi}{2} \zeta_1 \right] \quad (h_o << z << h_1) \qquad (3\text{-}10)$$

The vector potential in this region can be determined from Equations (2-17) and (3-1). The resulting relation is

$$i\omega A_z = - \frac{\partial \psi}{\partial z} \left[1 - \frac{S^2(\rho)}{n^2} \right]^{-1} \qquad (3\text{-}11)$$

Since the second term in the square brackets is negligible in this region, the vector potential becomes

$$i\omega A_z \longrightarrow -F(\rho) \qquad (h_o << z << h_1) \qquad (3\text{-}12)$$

and therefore independent of altitude. Although it has not been demonstrated here, it can be shown that the vector potential remains essentially constant over the entire altitude range $0 \leq z << h_1$.

It now remains to construct a solution which obeys the proper boundary condition at the ground and has a region of validity in common with the solution just derived. As noted above, the boundary condition at the ground is that the horizontal electric field vanishes. The horizontal electric field is proportional to the scalar potential ψ, and therefore, by virtue of Equation (3-1), to $\partial A_z/\partial z$. Thus, the boundary condition at the ground is that $\partial A_z/\partial z$ vanishes there. With this boundary condition, a first integral of Equation (2-17) is

$$\frac{\partial A_z}{\partial z} = - n^2 k^2 \int_o^z \left[1 - \frac{S^2(\rho)}{n^2} \right] A_z dz \qquad (3\text{-}13)$$

If use is now made of the fact that A_z is essentially constant in the range $0 \leq z << h_1$, the quantity A_z may be taken outside the integral for values of the upper limit in this range. Combined with Equation (3-1), this leads to

$$\psi = - i\omega A_z(0,\rho) \left[z - \int_0^z \frac{S^2(\rho)}{n^2}\, dz \right] \qquad (3\text{-}14)$$

$$(z << h_1)$$

For $z >> h_o$, the integrand in Equation (3-14) becomes very small, and little error is made by extending the range of integration to infinity. Thus, in the range $h_o << z << h_1$, the potentials are given by

$$A_z = A_z(0,\rho) \qquad (3\text{-}15)$$

$$\psi = - i\omega A_z(0,\rho) \left[z - S^2(\rho) \int_0^\infty \frac{dz}{n^2} \right] \qquad (3\text{-}16)$$

$$(h_o << z << h_1)$$

The horizontal electric and magnetic fields derived from Equation (3-15) and (3-16) must be made to agree with those derived from Equation (3-12) and (3-13) by an adjustment of the parameter $S(\rho)$. This is most easily accomplished by making the ratio of the horizontal electric and magnetic fields, or the wave impedance, identical in the two cases. It can easily be shown that the horizontal electric field is proportional to ψ and the horizontal magnetic field is proportional to A_z. Thus, the impedance

$$Z(z,\rho) = \frac{E_\rho(z,\rho)}{B_\phi(z,\rho)} \sim \frac{\psi(z,\rho)}{A_z(z,\rho)} \qquad (3\text{-}17)$$

and the requirement that the impedances be identical for the two solutions results in the condition

$$S^2(\rho) = \frac{(h_1 + \frac{i\pi}{2}\zeta_1)}{\int_0^\infty \frac{dz}{n^2(z,\rho)}} \tag{3-18}$$

For any given index of refraction profile, the eigenvalue $S(\rho)$ can now be calculated from Equation (3-18) in a straightforward manner. However, it is possible to carry the approximate method one step further. The integrand in Equation (3-18) becomes very small at altitudes very much above the height h_o where

$$\sigma(h_o) = \varepsilon_o \omega \tag{3-19}$$

Furthermore, the integrand is essentially unity up to a conductivity scale height or so below this altitude. Therefore, an adequate approximation to the integral can be obtained by writing the index of refraction as

$$n^2 = 1 + ie^{(z-h_o)/\zeta_o} \tag{3-20}$$

where $\zeta_o(\rho)$ is the conductivity scale height at the altitude $h_o(\rho)$. The integral in Equation (3-18) can now be evaluated analytically, with the result

$$S^2(\rho) = \frac{(h_1 + \frac{i\pi}{2}\zeta_1)}{(h_o - \frac{i\pi}{2}\zeta_o)} \tag{3-21}$$

The above is an approximate analytic expression for the eigenvalue with which it is now possible to integrate Equation (2-20) in a rapid and straightforward manner. As mentioned earlier, the exact eigenvalue $S(\rho)$ is that which would be obtained for a laterally homogeneous medium with the local vertical conductivity profile. A number of full-wave solutions have been obtained numerically by E. C. Field [6] for a variety of conductivity profiles corresponding to normal and disturbed ionospheres. In Table 1, the eigenvalues obtained by Field are compared with those calculated from Equation (3-21) based on values of h_1, ζ_1, h_o, and ζ_o determined from Field's conductivity profiles. It can be seen that the agreement is excellent for the real part of $S(\rho)$ and quite good for the imaginary part. In view of the basic uncertainties in conductivity profiles, the use of the approximation derived above seems well justified.

Table 1. Calculated Phase Velocities and Attenuation Rates for a Laterally Homogeneous Ionosphere

Γ	v/c [EQ.(3-21)]	v/c (EXACT)	dB/1000 km [EQ.(3-21)]	dB/1000 km (EXACT)
10^{-7}	.58	.59	1.7	1.8
10^{-8}	.61	.61	1.7	1.8
10^{-9}	.65	.65	1.9	1.9
10^{-10}	.69	.69	2.0	2.0
10^{-11}	.73	.74	2.0	1.95
10^{-12}	.79	.79	1.8	1.6
10^{-13}	.81	.805	1.1	1.2
10^{-14}	.81	.805	0.81	0.90

Comparison of approximate phase velocities and attenuation rates, calculated using approximate Equation (3-21), with Field's exact solutions [6]. In both cases the conductivity profiles generated by Field are used. The parameter Γ is an ionization intensity parameter defined as $\Gamma = (FY)/R^2 t^{1.2}$, where FY is the total fission yield in megatons, t is the time after burst in seconds, and R is the radius in kilometers over which the debris is assumed to be spread uniformly.

SECTION IV

SCATTERING BY A CYLINDRICALLY SYMMETRIC DISTURBANCE

The formalism developed in the preceding sections will now be applied to the calculation of the effect of a localized cylindrically-symmetric ionospheric disturbance on the radiated field of an ELF transmitter. The applicability of the theory requires that lateral gradients be small; in particular, the disturbed region must join continuously, at its outer boundary, with the undisturbed region. The undisturbed region is assumed to be horizontally stratified.

The geometry of transmitter, disturbance, and receiver is shown in plan view in Figure 1. For simplicity, the transmitter and receiver have been assumed to be located in the undisturbed portion of the waveguide. The coordinates (r,θ) are plane polar coordinates referred to the transmitter, while (ρ,ϕ) are plane polar coordinates referred to the axis of the disturbance. The quantities to be calculated are the field amplitudes at the receiver with and without the disturbance.

Near the ground, the vector potential is a function $g(\rho,\phi)$ of the lateral coordinates satisfying Equation (2-20). The function $g(\rho,\phi)$ in the undisturbed region must satisfy the same equation with $S = S_o$. Thus, the problem may be regarded as the two-dimensional scattering by a cylindrically-symmetric complex "potential" $V(\rho) = S^2(\rho) - S_o^2$.

In the undisturbed region, $g(\rho,\phi)$ can be decomposed into two parts, one of which represents the incident wave and the other the scattered wave. Thus, $g(\rho,\phi)$ can be written

$$g(\rho,\phi) = g^i + g^s(\rho,\phi) \qquad (4\text{-}1)$$

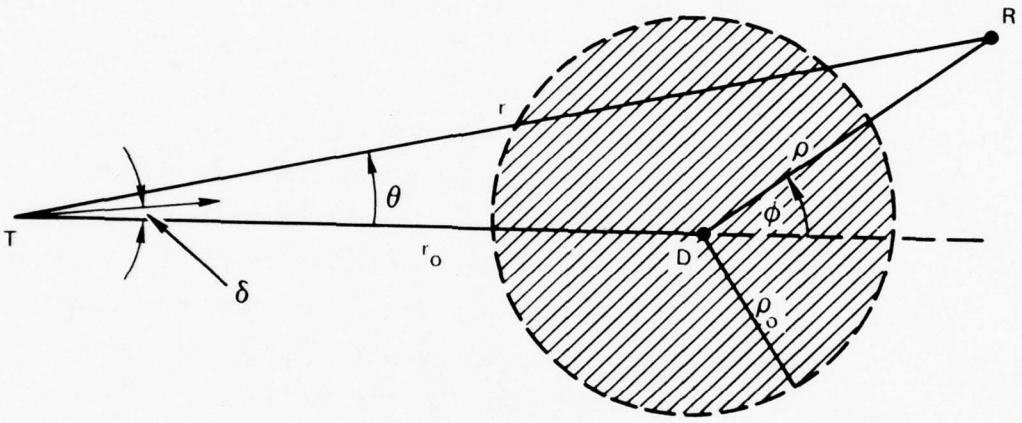

Figure 1. Coordinate System and Geometry of Transmitter (T), Receiver (R), and Disturbed Region of Waveguide (Shaded Area Centered at D)

The function g^i is the transverse factor of Equation (1-1), with α replaced by $(\theta-\delta)$, i.e.,

$$g^i(r,\theta) = \cos(\theta-\delta) H_1^{(1)}(kS_o r) \tag{4-2}$$

By use of Graf's addition theorem for Bessel functions [7], g^i can be expanded, in the region $\rho_o \leq \rho \leq r_o$, in functions of the (ρ,ϕ) coordinates. The result is

$$g^i(\rho,\phi) = \sum_{m=0}^{\infty} \varepsilon_m J_m(kS_o\rho)\left[\alpha_m \cos(m\phi) + \beta_m \sin(m\phi)\right]$$

$$(\rho_o \leq \rho \leq r_o) \tag{4-3}$$

where

$$\varepsilon_o = 1/2$$

$$\varepsilon_m = 1 \qquad (m \neq 0)$$

$$\alpha_m = (-1)^m \cos\delta\left[H_{m+1}^{(1)}(kS_o r_o) - H_{m-1}^{(1)}(kS_o r_o)\right]$$

$$\beta_m = (-1)^{m+1} \sin\delta\left(\frac{2m}{kS_o r_o}\right) H_m^{(1)}(kS_o r_o) \tag{4-4}$$

The radial function $g^s(\rho,\phi)$ must be a solution of Bessel's equation corresponding to outgoing waves at large radial distance. The general outgoing wave solution can be written in the form

$$g^s(\rho,\phi) = \sum_{m=0}^{\infty} \varepsilon_m H_m^{(1)}(kS_o\rho)\left[\gamma_m^{(1)}\alpha_m \cos(m\phi) + \gamma_m^{(2)}\beta_m \sin(m\phi)\right]$$

$$(\rho \geq \rho_o) \tag{4-5}$$

where $\gamma_m^{(1)}$ and $\gamma_m^{(2)}$ are constants yet to be determined. From Equation (4-3) and (4-5), the total radial function in the region $\rho_o \leq \rho \leq r_o$ is

$$g(\rho,\phi) = \sum_{m=0}^{\infty} \varepsilon_m \left[g_m^{(1)}(\rho)\cos(m\phi) + g_m^{(2)}(\rho)\sin(m\phi) \right] \qquad (4\text{-}6)$$

where

$$g_m^{(1)}(\rho) = \alpha_m \left[J_m(kS_o\rho) + \gamma_m^{(1)} H_1^{(1)}(kS_o\rho) \right]$$

$$g_m^{(2)}(\rho) = \beta_m \left[J_m(kS_o\rho) + \gamma_m^{(2)} H_1^{(1)}(kS_o\rho) \right] \qquad (4\text{-}7)$$

$$(\rho_o \leq \rho \leq r_o)$$

In order to complete the solution, it is necessary to solve the wave equation in the disturbed region, subject to appropriate boundary conditions at $\rho = 0$ and $\rho = \rho_o$. The function $g(\rho,\phi)$ must be a solution of Equation (2-20), the general form of which is given by Equation (4-6). The functions $g_m^{(1),(2)}(\rho)$ satisfy the equation

$$\frac{1}{\rho}\frac{d}{d\rho}\left(\rho \frac{dg_m}{d\rho}\right) + \left[k^2 S^2(\rho) - \frac{m^2}{\rho^2}\right] g_m = 0 \qquad (4\text{-}8)$$

$$(\rho \leq \rho_o)$$

(It will be understood that the omission of a superscript implies both superscripts.)

The boundary conditions at $\rho = \rho_o$ are that the electric and magnetic fields must be continuous there. It can easily be verified that, with $S^2(\rho)$ continuous at $\rho = \rho_o$, all the

continuity requirements can be satisfied by making g_m and $dg_m/d\rho$ continuous at $\rho = \rho_o$.

The boundary condition at $\rho = 0$ is that all the fields remain finite, which in turn requires $g_m(0)$ and $g_m'(0)$ to be finite. This boundary condition can be conveniently formalized by transforming Equation (4-8) into a Ricatti-type equation. First one lets

$$g_m(\rho) = \bar{\rho}^m \, U_m(\bar{\rho}) \tag{4-9}$$

where

$$\bar{\rho} = \rho/\rho_o$$

The function $U(\bar{\rho})$ then satisfies

$$U_m'' + \frac{(2m+1)\,U_m'}{\bar{\rho}} + \bar{k}^2 S^2 U_m = 0 \tag{4-10}$$

where

$$\bar{k} = k\rho_o$$

If one then introduces as the variable

$$Y_m = - \bar{\rho}^{(2m+1)} \frac{U_m'}{U_m} \tag{4-11}$$

Equation (4-10) becomes

$$Y_m' = \bar{k}^2 S^2(\bar{\rho})\,\bar{\rho}^{(2m+1)} + \frac{Y_m^2}{\bar{\rho}^{(2m+1)}} \tag{4-12}$$

This equation can be integrated outward from the origin in a straightforward manner once the behavior of Y_m at the origin is known. This can be deduced from the requirement that $g_m(0)$ and $g_m'(0)$ are finite. In the neighborhood of $\rho = 0$, $S^2(\rho)$ is approximately constant, and Equation (4-8) reduces to Bessel's equation. The solution which is finite at the origin varies with ρ as

$$g_m \approx \rho^m [1 + 0(\rho^2)] \qquad \rho \to 0 \qquad (4\text{-}13)$$

Thus, from Equation (4-9) and (4-11)

$$Y_m(\bar{\rho}) \approx \bar{\rho}^{2(m+1)} \qquad \rho \to 0 \qquad (4\text{-}14)$$

so that

$$Y_m(0) = Y_m'(0) = 0 \qquad (4\text{-}15)$$

The last condition is sufficient to start an outward numerical integration of Equation (4-12), from which one obtains a value $Y_m(1)$ at the boundary $\rho = \rho_o$.

Finally, the constants $\gamma_m^{(1)}$ and $\gamma_m^{(2)}$ in Equation (4-7) can now be determined from the boundary conditions at $\rho = \rho_o$. Since $g_m(\rho)$ and $g_m'(\rho)$ must be continuous at $\rho = \rho_o$, their ratio must also be continuous. In the undisturbed region, the ratio is calculated from Equation (4-7), and in the disturbed region from Equation (4-9) and (4-11). The resulting relation, for either superscript, is

$$kS_o\rho_o \frac{\left[J_m'(kS_o\rho_o) + \gamma_m H_m^{(1)'}(kS_o\rho_o)\right]}{\left[J_m(kS_o\rho_o) + \gamma_m H_m^{(1)}(kS_o\rho_o)\right]} = m - Y_m(1) \qquad (4\text{-}16)$$

The constants $\gamma_m^{(1)}$ and $\gamma_m^{(2)}$ are clearly the same, and with a little further manipulation, can be shown to be given by

$$\gamma_m = \frac{\left[J_m(kS_o\rho_o)Y_m(1) - kS_o\rho_o J_{m+1}(kS_o\rho_o)\right]}{\left[kS_o\rho_o H_{m+1}^{(1)}(kS_o\rho_o) - Y_m(1)H_m^{(1)}(kS_o\rho_o)\right]} \qquad (4\text{-}17)$$

Combined with Equation (4-5), this gives

$$g^s(\rho,\phi) = \sum_{m=0}^{\infty} \varepsilon_m \gamma_m H_m^{(1)}(kS_o\rho)\left[\alpha_m \cos(m\phi) + \beta_m \sin(m\phi)\right] \qquad (4\text{-}18)$$

which now enables one to calculate the scattered amplitude everywhere.

SECTION V

CALCULATION OF SCATTERED MAGNETIC FIELD

In ELF reception by receivers submerged in the ocean, the receiving antenna measures the horizontal electric field. The horizontal electric field at any depth in the ocean can be determined from the horizontal magnetic field at the surface. It is therefore the latter quantity which will be calculated explicitly here.

It can be expected that an ionospheric disturbance will have its greatest effect when its axis passes through the transmitter-receiver line. Consequently, it will be assumed that $\theta = 0$ and $\phi = 0,\pi$ (see Figure 1). Furthermore, it will be assumed that the transmitter is oriented for maximum signal at the receiver, so that $\delta = 0$. These assumptions, in addition to applying to the case of greatest practical interest, also simplify the calculation somewhat. However, the generalization to arbitrary configuration of transmitter, receiver, and disturbance is straightforward.

For the configuration described above, the horizontal magnetic field can be shown to have only an azimuthal component. The azimuthal magnetic field is related to the vector potential by

$$B_\phi = - \frac{\partial A_z}{\partial \rho} \qquad (5\text{-}1)$$

Aside from an excitation factor, the total azimuthal magnetic field is therefore

$$B_\phi \sim \sum_{m=0}^{\infty} (-1)^m \varepsilon_m \alpha_m \frac{\partial g_m}{\partial \rho} \qquad (5\text{-}2)$$

$$(r < r_o)$$

$$B_\phi \sim \sum_{m=0}^{\infty} \varepsilon_m \alpha_m \frac{\partial g_m}{\partial \rho} \qquad (5\text{-}3)$$

$$(r \geq r_o)$$

where α_m is given by Equation (4-4) with $\delta = 0$. (The factor $(-1)^m$ which appears in Equation (5-2) arises from the factor $\cos(m\phi)$ in Equation (4-6), in which $\phi = \pi$ for $r < r_o$.) The azimuthal field of the incident wave is given by

$$B_\phi^i \sim \frac{\partial}{\partial \rho} H_1^{(1)}(kS_o r) \qquad (5\text{-}4)$$

$$r = r_o \mp \rho$$

with the upper sign corresponding to Equation (5-2) and the lower sign to Equation (5-3).

The evaluation of $\frac{\partial g_m}{\partial \rho}$ in Equation (5-2) and (5-3) depends on whether the receiver is inside or outside the disturbed region. If the receiver is outside the disturbed region $(\rho > \rho_o)$,

$$g_m(\rho) = \gamma_m H_m^{(1)}(kS_o\rho) + J_m(kS_o\rho) \qquad (5\text{-}5)$$

where γ_m is calculated from Equation (4-17) after an integration of Equation (4-12) from $\bar{\rho} = 0$ to $\bar{\rho} = 1$. The quantity $\frac{\partial g_m}{\partial \rho}$ can then be calculated by a straightforward differentiation of Equation (5-5).

If the receiver is inside the disturbance $(\rho \leq \rho_o)$, one additional integration is required to determine $\frac{\partial g_m}{\partial \rho}$. It is

easy to show from Equation (4-9) and (4-11) that g_m satisfies the differential equation

$$g_m'(\bar{\rho}) = g_m(\bar{\rho}) \left[\frac{m}{\bar{\rho}} + \frac{Y_m(\bar{\rho})}{\bar{\rho}^{2m+1}} \right] \qquad (5\text{-}6)$$

with the boundary condition (Equation (5-5))

$$g_m(1) = \gamma_m H_m^{(1)}(\bar{k}S_o) + J_m(\bar{k}S_o) \qquad (5\text{-}7)$$

The function $Y_m(\bar{\rho})$ can be tabulated during the same integration of Equation (4-12) from which γ_m is calculated. With γ_m and $Y_m(\bar{\rho})$ known, Equation (5-6) can be integrated inward from $\bar{\rho} = 1$ to determine $\frac{\partial g_m}{\partial \rho}$ anywhere inside the disturbance.

For a configuration in which the transmitter is under the center of the disturbance and the receiver is outside the disturbance, the field at the receiver can be obtained by interchanging the positions of transmitter and receiver, performing the calculation as described above, and invoking reciprocity.

SECTION VI

NUMERICAL RESULTS AND DISCUSSION

Illustrative calculations based on the preceding theory have been carried out for the disturbances resulting from a high-altitude, megaton-range nuclear explosion during daytime. The bomb fission yield was taken to be 2 MT and the fission products were assumed to rise to an altitude of 300 km at 1 min and 1000 km at 10 min after the burst. For both times, the ionization rate from delayed gamma rays was calculated as a function of altitude and distance from ground zero using standard formulas [8]. Ionization from delayed beta rays was neglected, since it depends on the local magnetic dip angle and is expected to have a smaller effect than the gammas.

The resulting electron and ion concentrations were calculated by R. Turco [9] assuming steady-state chemistry and including e^-, $NO^+.nH_2O$, $H_3O^+.nH_2O$, O_2^- and $NO_3^-.nH_2O$. Using mass-dependent ion mobilities [10] similar to those of Carroll and Mason [11], ionospheric conductivity profiles were computed [9]. From these results, the two altitudes and the two scale heights needed for the calculation of approximate eigenvalues (Equation (3-21)) at 45 Hz were determined. The results appear in Tables 2 and 3, the last entry in each table representing the beginning of ambient conditions. These tables were the input data for electromagnetic field calculations using the methods described in the preceding section.

In each case, the transmitter was located outside the disturbance at 1000 km from the nearest edge, and the electromagnetic field was calculated at points along the line between the transmitter and the center of the disturbance, ranging from 200 km from the transmitter to 1000 km beyond the far edge of the disturbance. (Larger transmitter-receiver distances would require earth-curvature corrections.) The fields

Table 2. Ionospheric Parameters and Approximate Eigenvalues for 2 MT of Fission Products at 300 km Altitude 1 Min After Burst Time

GROUND RANGE (km)	h_o (km)	ζ_o (km)	h_1 (km)	ζ_1 (km)	Re(S)	Im(S)
0	18.66	3.19	59.32	2.97	1.73	.30
200	19.60	3.18	60.22	2.92	1.71	.28
400	22.60	3.54	62.47	2.73	1.62	.25
600	25.19	3.44	63.88	2.78	1.56	.22
800	27.76	3.71	65.03	2.79	1.50	.21
1000	29.88	3.47	65.95	2.77	1.46	.18
1200	31.87	3.42	66.71	2.74	1.43	.17
1400	34.30	3.23	67.34	2.71	1.39	.15
1600	36.70	3.01	67.62	2.69	1.35	.13
1800	40.10	2.64	68.04	2.76	1.30	.11
2000	44.58	2.19	68.50	2.77	1.24	.087
2200	50.86	1.73	69.85	2.72	1.17	.067
2300	54.63	1.65	71.17	2.78	1.14	.062
2400	58.13	2.11	73.68	2.92	1.12	.067
2450	58.28	2.50	75.53	2.93	1.14	.073
2500	58.20	2.57	77.58	3.29	1.15	.078
2550	58.20	2.57	78.24	3.42	1.16	.080
2600	58.20	2.57	78.20	3.52	1.16	.081

Table 3. Ionospheric Parameters and Approximate Eigenvalues for 2 MT of Fission Products at 1000 km Altitude 10 Min After Burst Time

GROUND RANGE (km)	h_o (km)	ζ_o (km)	h_1 (km)	ζ_1 (km)	Re(S)	Im(S)
0	33.70	8.52	70.05	3.15	1.36	.31
200	33.81	8.49	70.08	3.16	1.36	.31
400	34.45	8.31	70.27	3.21	1.35	.30
700	35.80	8.14	70.67	3.33	1.34	.28
1000	37.29	8.39	71.11	3.47	1.31	.28
1500	40.00	7.15	71.77	3.71	1.30	.23
2000	41.88	6.66	72.38	4.01	1.28	.21
2600	44.13	5.34	73.10	4.12	1.27	.18
3200	47.13	3.90	73.72	4.20	1.24	.14
3400	49.12	3.12	73.90	4.21	1.22	.12
3500	50.44	2.68	73.99	4.22	1.21	.10
3600	52.23	2.28	74.12	4.20	1.19	.094
3800	57.21	1.87	75.69	3.86	1.15	.076
4400	58.20	2.57	78.19	3.52	1.16	.081

corresponding to the first ten partial waves were calculated, and superimposed to give the scattered field at any point. In all cases, only the lowest three or four partial waves were found to make an appreciable contribution at any field point.

In Figures 2 and 3 the attenuation of the 45-Hz electromagnetic field is plotted as a function of distance from the transmitter. The attenuation in the absence of the disturbance is also plotted for purposes of comparison at 1 min after the explosion (Figure 2); the radius of the disturbance is about 2600 km, and the ionosphere at the center has been lowered by 40 km. The additional attenuation across the entire disturbance is about 0.5 dB. At 10 min after the explosion (Figure 3) the radius of the disturbance is about 4400 km, the ionosphere at the center has been lowered by 25 km, and the additional attenuation is about 3 dB. In both cases, the field between the transmitter and the leading edge of the disturbance is essentially unaltered, indicating that there is little back-scattering.

It is interesting to compare these results of the full-wave solution with the "great-circle WKB" approximation which has been used in ELF calculations by Pappert and Moler [12] and others. This is essentially a two-dimensional approximation in which the properties of the waveguide are allowed to vary along the direction of propagation, but are assumed uniform in the perpendicular direction. The properties throughout the waveguide are assumed to be those of the great-circle path between transmitter and receiver. In this approximation, the magnetic field of the wave is given by

$$|B_\phi(r)| \sim \frac{1}{r^{1/2}} \frac{1}{\left[h_o^T h_o(r)\right]^{1/2}} |S^T S(r)|^{-1/4} \exp\left[-\int^r I_m(s)\,dr\right] \tag{6-1}$$

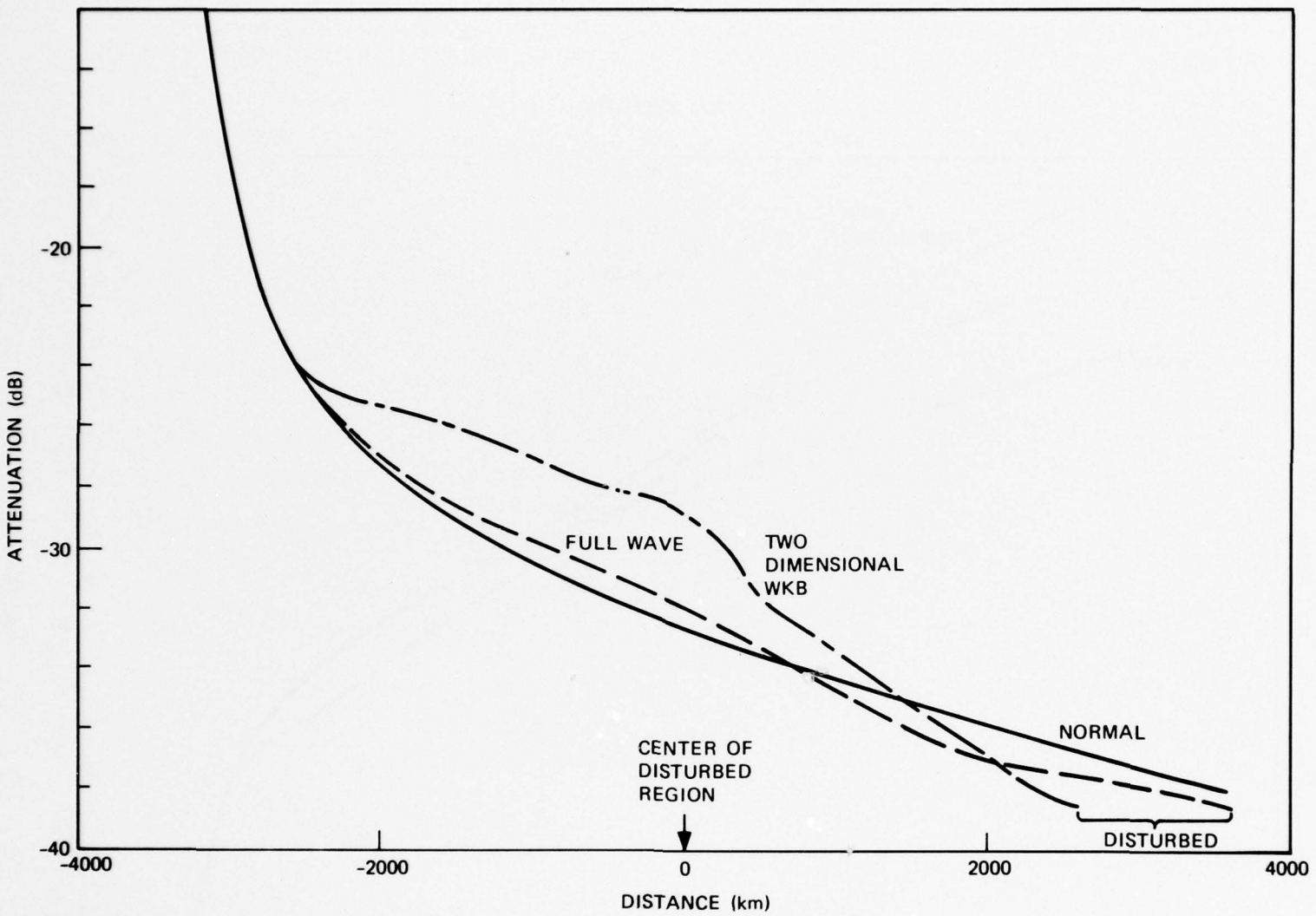

Figure 2. Attenuation of the Horizontal Electromagnetic Field (Arbitrary Reference Level) Along a Path from the Transmitter Through the Center of the Disturbed Region. The Radius of the Disturbed Region is 2600 km

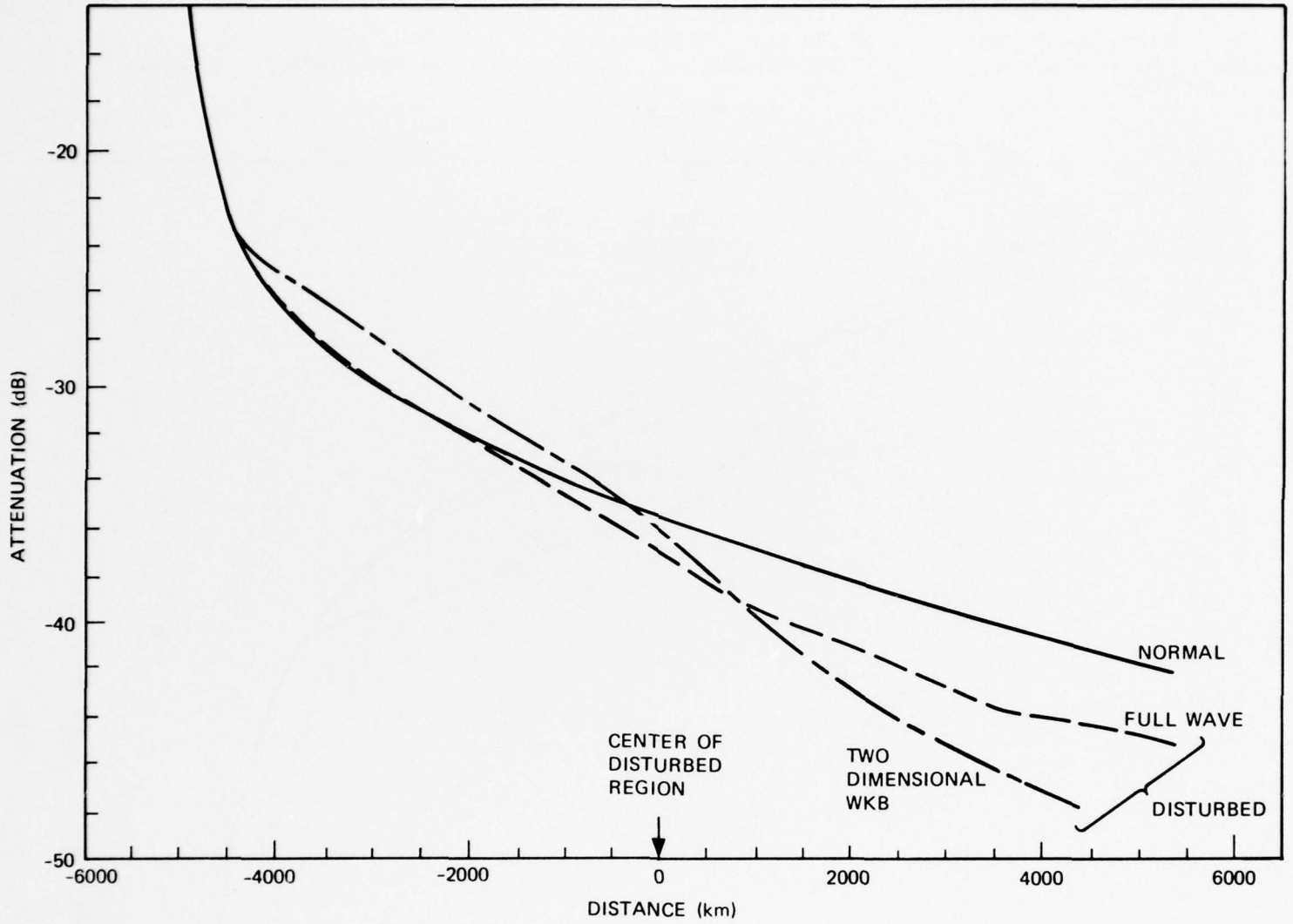

Figure 3. Attenuation of the Horizontal Electromagnetic Field (Arbitrary Reference Level) Along a Path from the Transmitter Through the Center of the Disturbed Region. The Radius of the Disturbed Region is 4400 km

where the superscript T denotes the transmitter location. The factor $[h_o(r)]^{-1/2}$ represents the increase or decrease in energy density as the height of the waveguide changes.

The attenuation calculated from this approximation is also shown in Figures 2 and 3. The approximation has been applied only to that portion of the path inside the disturbance, so that Equation (6-1) has been normalized to the undisturbed value at the leading edge. The results show that this approximation underestimates the attenuation in most of the disturbance region, but overestimates the attenuation at the far edge of the disturbance by about a factor of two. This behavior is not surprising, since the two-dimensional approximation forces the wave to go under the ionospheric depression, thus both compressing and absorbing it, while the realistic full-wave solution permits the radio wave to go around the depression.

LIST OF REFERENCES

1. D. D. Crombie, "The Effects of a Small Local Change in Phase Velocity on the Propagation of a VLF Radio Signal," Radio Sci. J. Res. NBS, Vol. 68D, 1964, p. 706.

2. J. R. Wait, Electromagnetic Waves in Stratified Media, Pergamon, New York, 1972.

3. J. Galejs, Terrestrial Propagation of Long Electromagnetic Waves, Pergamon, New York, 1972.

4. P. E. Krasnushkin, "On the Propagation of Long and Very Long Radio Waves Around the Earth," Nuovo Cimento, Suppl., Vol. 26, 1962, pp. 50-112.

5. T. J. Wilcox, Scattering of ELF Waves by Localized Ionospheric Perturbations, TRW Systems Group Internal Report TRW 4360.7.74-50, March 1974.

6. E. C. Field, private communication, 1976.

7. G. N. Watson, A Treatise on the Theory of Bessel Functions, Cambridge University Press, England, 1952, p. 361.

8. Aids for the Study of Electromagnetic Blackout, General Electric Company-TEMPO, DNA 3499H, 25 February 1975.

9. R. Turco, private communication, 1976.

10. J. Green and D. Dee, private communication, 1976.

11. D. I. Carroll and E. A. Mason, "The Theoretical Relationship between Ion Mobility and Mass," Proc. 19th Ann. Conf. on Mass Spect., May 1971, pp. 315-319.

12. R. A. Pappert and W. F. Moler, "Propagation Theory and Calculations at Lower Extremely Low Frequencies (ELF)," IEEE Trans. on Communications, v. COM-22, April 1974, pp. 438-451.

DISTRIBUTION LIST

DEPARTMENT OF DEFENSE

Director
Command Control Technical Center
ATTN: C-650, G. C. Jones
ATTN: C-650, W. Heidig
ATTN: C-312, R. Mason

Director
Defense Advanced Rsch. Proj. Agency
ATTN: Nuclear Monitoring Research
ATTN: Strategic Tech. Office

Defense Communication Engineer Center
ATTN: Code R220, M. Horowitz
ATTN: Code R410, James W. McLean
ATTN: Code 720, John Worthington

Director
Defense Communications Agency
ATTN: Code 810, R. W. Rostron
ATTN: Code 480
ATTN: Code 101B, Major Rood

Defense Communications Agency
WWMCCS System Engineering Org.
ATTN: R. L. Crawford

Defense Documentation Center
Cameron Station
12 cy ATTN: TC

Director
Defense Intelligence Agency
ATTN: DIAAP, Albert L. Wise
ATTN: DIAST-5
ATTN: DB-4C, Edward O'Farrell
ATTN: HQ-TR, J. H. Stewart
ATTN: DT-1BZ, Captain R. W. Morton

Director
Defense Nuclear Agency
ATTN: DDST
3 cy ATTN: RAAE
ATTN: STVL
3 cy ATTN: TITL, Tech. Library
ATTN: TISI, Archives

Dir. of Defense Rsch. & Engineering
Department of Defense
ATTN: S&SS (OS)

Commander
Field Command
Defense Nuclear Agency
ATTN: FCPR

Director
Interservice Nuclear Weapons School
ATTN: Document Control

Director
Joint Strat. Target Planning Staff, JCS
ATTN: JPST, Captain G. D. Goetz

DEPARTMENT OF DEFENSE (Continued)

Chief
Livermore Division, Field Command, DNA
Lawrence Livermore Laboratory
ATTN: FCPRL

Director
National Security Agency
ATTN: John Skillman, R52
ATTN: Oliver H. Bartlett, W32

OJCS/J-3
ATTN: WWMCCS, Eval. Ofc., Mr. Toma

DEPARTMENT OF THE ARMY

Commander/Director
Atmospheric Sciences Laboratory
US Army Electronics Command
ATTN: DRSEL-BL-SY-S, F. E. Niles

Commander
Harry Diamond Laboratories
ATTN: DRXDO-NP, Francis N. Wimenitz
ATTN: DRXDO-TI, Mildred H. Weiner

Director
US Army Ballistic Research Labs.
ATTN: Tech. Lib., Edward Baicy

Commander
US Army Electronics Command
ATTN: J. E. Quigley

Commander
US Army Foreign Science & Tech. Center
ATTN: P. A. Crowley
ATTN: R. Jones

Commander
US Army Materiel Dev. & Readiness Command
ATTN: DRCLDC, J. A. Bender

Commander
US Army Nuclear Agency
ATTN: MONA-WE, J. Berberet

DEPARTMENT OF THE NAVY

Chief of Naval Operations
Navy Department
ATTN: OP 943, LCDR Huff

Chief of Naval Research
Navy Department
ATTN: Code 420
ATTN: Code 461
ATTN: Code 402
ATTN: Code 421

Commanding Officer
Naval Intelligence Support Center
ATTN: Code 5404, J. Galet

DEPARTMENT OF THE NAVY (Continued)

Commander
Naval Ocean Systems Center
ATTN: William F. Moler
ATTN: R. Eastman
3 cy ATTN: Code 2200

Director
Naval Research Laboratory
ATTN: Code 7701, Jack D. Brown
ATTN: Code 5461, Trans. Inon. Prop.
ATTN: Code 5460, Electromag. Prop. Br.
ATTN: Code 5410, John Davis
ATTN: Code 5430, Satellite Comm.
ATTN: Code 5465, Prop Applications

Officer-in-Charge
Naval Surface Weapons Center
ATTN: Code WA501, Navy Nuc. Prgms. Off.

Commanding Officer
Navy Underwater Sound Laboratory
ATTN: Peter Bannister

Director
Strategic Systems Project Office
Navy Department
ATTN: NSP-2141

DEPARTMENT OF THE AIR FORCE

Commander
ADC/DC
ATTN: DC, Mr. Long

Commander
ADCOM/XPD
ATTN: XP
ATTN: XPQDQ

AF Geophysics Laboratory, AFSC
ATTN: OPR, James C. Ulwick
ATTN: OPR, Alva T. Stair
ATTN: SUOL, Rsch. Lib.
ATTN: PHP, Jules Aarons

AF Weapons Laboratory, AFSC
ATTN: DYC, John M. Kamm
ATTN: DYT, Capt L. Wittwer
ATTN: SUL

AFTAC
ATTN: TN
ATTN: TF/Maj Wiley

Air Force Avionics Laboratory, AFSC
ATTN: AAB, H. M. Hartman

Headquarters
Electronic Systems Division, (AFSC)
ATTN: James Whelan

Commander
Foreign Technology Division, AFSC
ATTN: ETD, B. L. Ballard

Hq. USAF/RD
ATTN: RDQ

DEPARTMENT OF THE AIR FORCE (Continued)

Commander
Rome Air Development Center, AFSC
ATTN: EMTLD, Doc. Library

SAMSO/MN
ATTN: MNNL, Lt Col Kennedy

SAMSO/SZ
ATTN: SZJ, Major Lawrence Doan
ATTN: SZ

Commander in Chief
Strategic Air Command
ATTN: NRT
ATTN: XPFS, Maj Brian G. Stephan
ATTN: Chief Scientist
ATTN: ADWATE, Capt Bruce Bauer

ENERGY RESEARCH & DEVELOPMENT ADMINISTRATION

Division of Military Application
US Energy Rsch. & Dev. Admin.
ATTN: Doc. Con. for Donald I. Gale

University of California
Lawrence Livermore Laboratory
ATTN: Glenn C. Werth, L-216
ATTN: Frederick D. Seward, L-46

Los Alamos Scientific Laboratory
ATTN: Doc. Con. for R. F. Taschek
ATTN: Doc. Con. for Donald R. Westervelt
ATTN: Doc. Con. for P. W. Keaton

Sandia Laboratories
Livermore Laboratory
ATTN: Doc. Con. for Thomas B. Cook, Org. 8000
ATTN: Doc. Con. for Byran E. Murphey

Sandia Laboratories
ATTN: Doc. Con. for A. Dean Thornbrough, Org. 1245
ATTN: Doc. Con. for Space Project Div.
ATTN: Doc. Con. for 3141, Sandia Rpt. Coll.

US Energy Rsch. & Dev. Admin.
Albuquerque Operations Office
ATTN: Doc. Con. for D. W. Sherwood

US Energy Rsch. & Dev. Admin.
Division of Headquarters Services
Library Branch G-043
ATTN: Doc. Con. for Allen Labowitz

OTHER GOVERNMENT AGENCIES

Department of Commerce
National Bureau of Standards
ATTN: Sec. Officer for Raymond T. Moore

Department of Commerce
Office of Telecommunications
Institute for Telecom Science
ATTN: D. D. Crombie
ATTN: William F. Utlaut
ATTN: L. A. Berry
ATTN: A. Glenn Jean

OTHER GOVERNMENT AGENCIES (Continued)

Department of Transportation
Office of the Secretary
ATTN: R. L. Lewis
ATTN: R. H. Doherty

DEPARTMENT OF DEFENSE CONTRACTORS

Aeronomy Corporation
ATTN: S. A. Bowhill

Aerospace Corporation
ATTN: Irving M. Garfunkel

Analytical Systems Engineering Corp.
ATTN: Radio Sciences

The Boeing Company
ATTN: J. F. Kenny
ATTN: Glenn A. Hall

University of California at San Diego
Marine Physical Lab. of the Scripps
Institute of Oceanography
ATTN: Henry G. Booker

ESL, Inc.
ATTN: James Marshall

General Electric Company
Space Division
Valley Forge Space Center
ATTN: M. H. Bortner, Space Sci. Lab.

General Electric Company
TEMPO-Center for Advanced Studies
ATTN: DASIAC
ATTN: B. Gambill
ATTN: Warren S. Knapp
ATTN: Don Chandler

Geophysical Institute
University of Alaska
ATTN: T. N. Davis
ATTN: Neal Brown
ATTN: Technical Library

GTE Sylvania, Inc.
Electronics Systems GRP-Eastern Div.
ATTN: Marshal Cross

Johns Hopkins University
Applied Physics Laboratory
ATTN: Document Librarian

DEPARTMENT OF DEFENSE CONTRACTORS (Continued)

Lockheed Missiles & Space Company, Inc.
ATTN: W. L. Imhof, D/52-12
ATTN: Richard G. Johnson, Dept. 52-12

Lowell Technol. Inst. Rsch. Foundation
ATTN: Dr. Bibl

M.I.T. Lincoln Laboratory
ATTN: James H. Pannell, L-246
ATTN: Lib. A-082 for David M. Towle

Mission Research Corporation
ATTN: F. Fajen
ATTN: R. Hendrick
ATTN: M. Scheibe

The Mitre Corporation
ATTN: G. Harding
ATTN: John Morganstern

Pacific-Sierra Research Corp.
ATTN: E. C. Field, Jr.

Pennsylvania State University
Ionosphere Research Laboratory
ATTN: Ionospheric Research Lab.

R & D Associates
ATTN: R. P. Turco
ATTN: H. A. Ory
ATTN: Forrest Gilmore
ATTN: William J. Karzas
ATTN: Bryan Gabbard
ATTN: Carl Greifinger
ATTN: Phyliss Greifinger

The Rand Corporation
ATTN: Cullen Crain

Stanford Research Institute
ATTN: George Carpenter
ATTN: Gary Price
ATTN: Walter G. Chestnut
ATTN: Donald Neilson
ATTN: James R. Peterson

TRW Defense & Space Sys. Group
ATTN: Dianna Dee
ATTN: Saul Altschuler